Biomed Microdevices (2015) 17:5
DOI 10.1007/s10544-014-9925-6

A giant magnetoimpedance-based biosensor for sensitive detection of Escherichia coli O157:H7

Zhen Yang · Xue-cheng Sun · Tao Wang · Chong Lei · Yan Liu · Yong Zhou · Jian Lei

Abstract A giant magnetoimpedance (GMI)-based biosensor was developed for detection of Escherichia coli (E. coli) O157:H7. The GMI sensor involving the sensing elements of Cr/Cu/NiFe/Cu/NiFe was fabricated by Micro Electro-Mechanical system (MEMS) technology, including thick photoresist lithography and electroplating. A separate Au film substrate as immunoplatform was used to capture E. coli O157:H7. The monoclonal mouse anti-E. coli antibody was immobilized on Au film substrate surface with a self-assembled layer. The different concentration E. coli O157:H7 (100, 300 and 500 cfu/ml) were combined with Dynabeads-antibody conjugates (DAC) respectively. DAC were prepared by conjugating streptavidin-coupled Dynabeads with biotin-labeled polyclonal mouse anti-E. coli antibodies. The classical sandwich assay was used for detection of E. coli O157:H7 targeted with Dynabeads by using antibody-antigen pair combination of biotin-streptavidin. The fundamental principle for detection of E. coli O157:H7 based on GMI sensor was that Dynabeads were employed as magnetic labels of E. coli O157:H7, and E. coli O157:H7 can be monitored by detecting the fringe field of Dynabeads using magnetic sensing elements. We observed that the GMI ratio were significantly improved due to the presence of E. coli O157:H7 combined with Dynabeads. The GMI ratio increased as the E. coli O157:H7 concentration increased. A lower detectable concentration of 100 cfu/ml was achieved in present work. The GMI-based biosensor provides a new method to rapid and sensitive detection E. coli O157:H7, which has a large potential for bio-application.

Z. Yang · X.-c. Sun · T. Wang · C. Lei (✉) · Y. Liu · Y. Zhou (✉) · J. Lei
Key Laboratory for Thin Film and Microfabrication of the Ministry of Education, Department of Micro/Nano Electronics, School of electronic information and electrical engineering, Shanghai Jiao Tong University, Dongchuan Road 800, Shanghai 200240, People's Republic of China
e-mail: leiqhd@sjtu.edu.cn
e-mail: yzhou@sjtu.edu.cn

Published online: 28 January 2015

Keywords E. coli O157:H7 · Giant magnetoimpedance · Biosensor · Dynabeads · Au film

1 Introduction

The detection of pathogenic bacteria is vital for food safety, clinical diagnosis and therapies, portable water, and prevention strategies to combat bioterrorism agents. Among the different types of bacterial pathogens, Escherichia coli (E. coli) O157:H7 is one of the most dangerous food pathogens, which can cause serious foodborne illnesses such as hemorrhagic colitis and hemolytic uremic syndrome (Phillips 1999; Ivniski et al. 1999; Bunchnan and Dolye. 1997; Yu et al. 2001). It has been reported E. coli O157:H7 is responsible for an estimated 73,000 cases of infection and 61 deaths that occur in the United States each year (CDC 2005). Therefore, developing new techniques for rapid and sensitive detection of E. coli O157:H7 is extremely important to prevent catastrophic outbreaks. Traditional methods for the detection of trace amounts of bacteria require amplification or enrichment of the target bacteria in the sample (Phillips 1999; Gracias et al. 2004; Iqbal et al. 2000; Silk and Donnelly 1997). These methods tend to be laborious, time-consuming, costly and requires highly trained personnel, thereby delaying the results and making timely prevention of epidemic outbreaks difficult.

Until recently, some immunobiosensors have been reported as alternatives to the conventional methods. These immunobiosensor usually consists of two processes, a molecular recognition process, for sensing the specific antigen-antibody binding reaction at the surface of receptor, and the signal-transfer process, for responding to changes in an optical, spectroscopic, electrochemical, or electrical parameter of the receptor caused by the specific binding. The basis of the immunobiosensors is the interaction between the antigen of

the target cell and a surface-immobilised antibody. This antigen-antibody interaction can be detected using surface plasmon resonance (SPR) (Wink et al. 1998; Mayo and Hallock 1989), quartz crystal microbalance (QCM) (Skottrup et al. 2008), electrochemical impedance (Yang and Bashir 2008), optical coupling (Demarco et al. 1999), chemiluminescence (CL) biosensor (Wolter et al. 2008), capacitance affinity sensors (Berggren et al. 1998), amperometric immunosensors (Tang et al. 2002; Wang et al. 1998) and by various magnetic methods (Varshney et al. 2007; Ruan et al. 2002; Chen et al. 2011; Wang et al. 2014a, b). Although these techniques can directly measure antibody-antigen binding at the surface of the transducer, the lower sensitivity of these direct immunosensors limit their practical application in clinical and environmental assays. Sensitivity can be improved by a pre-concentration step. Rapid bacteria detection with magnetic beads by using an organic substrate based magnetoresistive sensor based on the classical sandwich assay format is achieved by Oh (Oh et al. 2013).

The giant magnetoimpedance (GMI) effect is a change in the complex impedance at high frequency (usually >0.1 MHz) and arises from the magnetic field-induced change of the dynamic relative permeability μ_r of the magnetic material. Recently, GMI has been observed in soft amorphous ferromagnetic wires (Atalay et al. 2006; Panina and Mohri 1994; Vázquez et al. 1997), thin film (Sommer and Chine 1995; Makhnovskiy et al. 2000; Zhou et al. 2001), and ribbons (Phan et al. 2006; Makhotkina et al. 1991; Alves et al. 2008) due to its possible application in the developing of the high sensitive magnetic sensor. The GMI-based magnetic sensors have several advantages, such as smaller size, quick response, high sensitivity, high stability and lower cost. The GMI sensors have been introduced into the field of biosensing as a biosensor prototype (Kurlyandskaya et al. 2003; Chen et al. 2011; Wang et al. 2014a, b) in order to develop a new generation of bioanalytical system.

In this paper, a GMI-based biosensor was developed for detection of E. coli O157: H7. The GMI sensor involving the sensing elements of Cr/Cu/NiFe/Cu/NiFe was fabricated by Micro Electro-Mechanical system (MEMS) technology, including thick photoresist lithography and electroplating. The different concentration E. coli O157:H7 (100, 300 and 500 cfu/ml) samples were prepared on a separate Au film substrate. The classical sandwich assay was used for detection of E. coli O157:H7 targeted with Dynabeads by using antibody-antigen pair combination of biotin-streptavidin. The GMI responses were observed for two states: with and without E. coli sample. The difference between the GMI responses can be used to determine the presence and level of the E. coli. The fundamental principle for detection of E. coli O157:H7 based on GMI sensor was that Dynabeads were employed as magnetic labels of E. coli O157:H7, and E. coli O157:H7 can be monitored by detecting the fringe field of Dynabeads using magnetic sensing elements. The research on the rapid and sensitive detection of E. coli O157:H7 using a GMI-based biosensor has not been reported.

2 Materials and methods

2.1 Chemicals and reagents

11-mercaptoundecanoic acid (11-MUA) was purchased from Aladdin Chemistry Co. Ltd (USA). 1-ethyl-3-[3-dimethylaminopropyl] carbodiimide (EDC) hydrochloride was purchased from Aladdin Chemistry Co. Ltd (USA). N-Hydroxysuccinimide (NHS) was purchased from Medpep (Shanghai Medpep Co. Ltd.). Phosphate buffer tablets (PBS PH 7.4) were purchased from Medicago AB (Uppsala, Sweden). Albumin from bovine serum (BSA) was purchased from Via-gene pro bio Technologies Co. ltd. (Shanghai, China). Deionized water was used to prepare phosphate buffered solution.

2.2 E. coli O157:H7 antibodies, antigens and Dynabeads

A mouse anti-E. coli O157:H7 monoclonal antibody, a biotin-conjugated anti-E. coli polyclonal antibody, E. coli antigen and shigella were purchased from Prajna Biology Technique Co. ltd. (Shanghai, China). The Dynabeads® MyOne™ Streptavidin C1 were purchased from Invitrogen, and were uniform, superparamagnetic beads of 1.0 μm in diameter with streptavidin monolayer covalently coupled to the hydrophilic bead surface.

2.3 Design and fabrication of GMI sensor

The photograph of the fabricated GMI sensor was shown in Fig. 1. The length of the straight line segment in the tortuous structure was 5 mm. The total turn number was 10. The widths of NiFe and Cu film were 140 and 100 μm respectively. The space between neighbor segments was 60 μm. The thicknesses of NiFe and Cu film were about 3 and 2 μm, respectively. The area of electrode was 2 mm×3 mm. The total area of sensing elements was 5 mm×3.94 mm.

The manufacturing process had been reported elsewhere (Wang et al. 2013, 2014a, b). It can be depicted briefly as follows: a) the 100 nm thick Cr/Cu seed layer was deposited on a glass substrate by radio frequency magnetron sputtering. b) Photoetching. c) The bottom NiFe layer was coated by electrodeposition. d) The Cu layer was accomplish with similar process e) the top NiFe layer was got. f) The seed layer was removed by reactive ion etching. The preparation process of high-integrated GMI sensor was shown in Fig. 2.

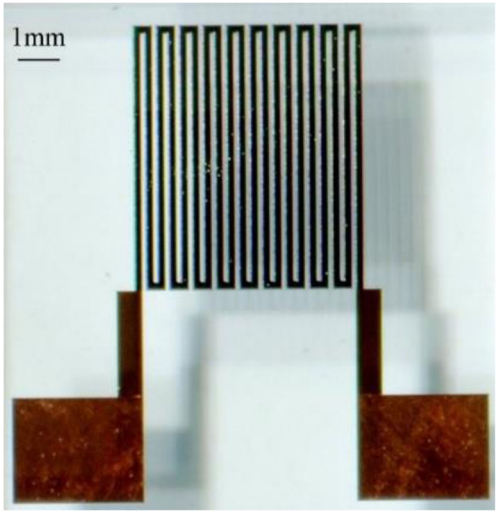

Fig. 1 Photograph of the fabricated GMI sensor

2.4 Magnetization characteristics

Figure 3 showed the magnetization curves of the electroplated NiFe film. One can find that the electroplated NiFe film had very good soft magnetic characteristics involving high saturation magnetization, clear easy axis and hard axis.

2.5 Preparation and modifying of the gold substrate

Gold substrates were prepared by deposition of Au film (300 nm) on a glass wafer by sputtering. After that, a photoresist layer was spun on the Au layer and patterned to several rectangles with dimensions of 5×3 mm, then the uncovered part of the Au layer was removed by reactive ion etching in the mixed solution (KI: I_2: H_2O—4 g: 2 g: 10 ml). The wafer was sliced into several chips each of which had one Au film on it.

First the Au films were bathed in 1 mol L^{-1} NaOH solution and 1 mol L^{-1} HCl in turn for 10 min, and then the Au films were rinsed with deionized water and alcohol, at last it was dried using a stream of nitrogen gas. Next the Au films were bathed in 30 mmol L^{-1} 11-mercaptoundecanoic acid at the room temperature for 3 h and washed twice with anhydrous alcohol and dried. Then the gold substrates were immersed and activated in a mixture obtained by dissolving EDC and NHS in PBS solution (PH=7.4) for1 h. The contents of EDC and NHS in this mixture were 0.2 mol L^{-1} and 0.05 mol L^{-1}, respectively. After that, the gold substrates were washed several times with PBS solution (PH=7.4).

The mouse anti-E.coli O157:H7 monoclonal antibody was immobilized onto the gold films surface through the linkage between their amino groups and the active epoxy groups on the self-assembly monolayer. Ten microliters of 1 mg.mL^{-1} anti-E. coli O157:H7 antibody solution was spread onto the gold substrate surface. The gold substrates were incubated at 4 °C in the freezer overnight. After incubation, the gold films were rinsed with phosphate buffered solution (PBS) and deionized water to remove physically absorbed antibodies. Finally, the gold films were sealed with 100 μl BSA solution (including 1 % BSA, 0.2 % tween 20) at 4 °C for 2 h and washed twice with PBS solution (PH=7.4).

2.6 Preparation of E. coli-Dynabeads complexes and bonding on the Au film

Biotinylated anti-E. coli polyclonal antibodies were conjugated with Dynabeads MyOne™ Streptavidin C1 (DMS). DMS were supplied as a suspension of 10 mg (approx. 7–12×10^9 particles) Dyanbeads per milliliter. 100 μl of the biotinylated anti-E. coli antibody (1 mg/ml stock concentration) were added to the Dynabeads solution (100 μl, 100 μg/ml); then, the mixture was allowed to incubate at 37 °C for 40 min with gentle shaking. After conjugation, the mixture was washed three times with 800 μl PBS with an intermitten magnetic separation. After the final washing, the Dynabeads (10^7) were resuspended in 1 ml of the same (wash) solution and stored at 4 °C for use.

Serial dilutions of pure culture of E. coli O157: H7 (100, 300, 500 cfu/mL) were prepared in PBS (0.01 M, pH 7.4)

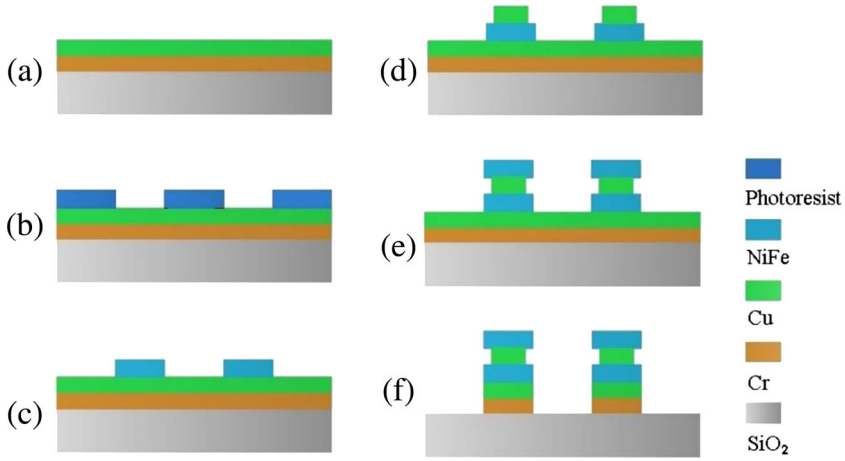

Fig. 2 Fabrication steps of the GMI sensor

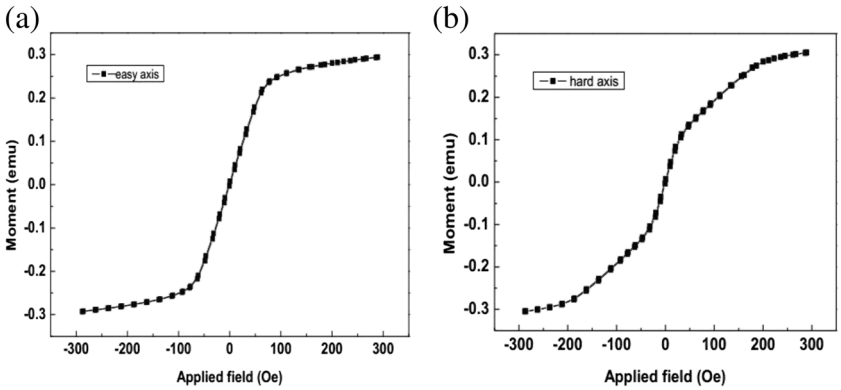

Fig. 3 The hysteresis loop of NiFe alloy: **a** easy axis; **b** hard axis

buffer. A 1 ml of pure culture was mixed with 40 μl of Dynabeads-antibody conjugates (DAC) for an immunoreaction time of 1 h at 37 °C. And then the E. coli-Dynabeads complexes were washed three times with 200 μl PBS with an intermittent magnetic separation. After the final washing, 40 μl of different suspensions were reserved and deposited on the antibody immobilized Au films for 20 min. After washing and drying. Different concentration E. coli samples were got and used for detection. The specificity test was in accordance with that of sensitivity test except that shigella was used instead of E. coli O157: H7. The preparation process of E. coli-Dynabeads was shown in Fig. 4.

2.7 Characterizations of E. coli-conjugated Dynabeads

Scanning electron microscopy (SEM) was used to observe the E. coli-conjugated Dynabeads and shigella-Dynabeads as seen in Fig. 5. The shigella-Dynabeads complexes was bond on the mouse anti-E. coli O157:H7 monoclonal antibody modified Au film for 20 min, and then washed with PBS. After the final washing, we found that almost all Dynabeads were removed as can be seen in the Fig 5d. From the Fig.5a.b.c, it was clear that the numbers of Dynabeads increased with increasing E. coli concentration. The SEM observations confirmed that Dynabeads-labeled E. coli was immobilized on the Au film.

2.8 Detection of E. coli O157:H7 based GMI measuring method

The detection of E. coli was based on a chemical conjugation of the magnetic beads and E. coli. The basic principle on which the E. coli detection based was that Dynabeads were employed as magnetic labels of E. coli, and E .coli can be monitored by detecting the fringe field of the Dynabeads using magnetic sensing elements, as was shown in Fig. 6. According to the above statement, the GMI ratio would not change, when the sample that shigella was used instead of E. coli O157: H7 was placed on the surface of GMI sensor. Different concentration E. coli samples (100, 300 and 500 cfu/ml) were placed on the surface of GMI sensor respectively. The GMI responses were measured by an impedance analyzer (E4991A). An external magnetic field (H_{ex}) of 0–60 Oe was applied along the longitudinal direction of the sample in order to induce strong changes in the skin depth. The relative change in impedance (GMI ratio) was defined as: GMI ratio (100 %) =100 %×[Z(H)-Z(H_0)]/Z(H_0), where Z(H) and Z(H_0) are the magnetoimpedance with and without magnetic field respectively.

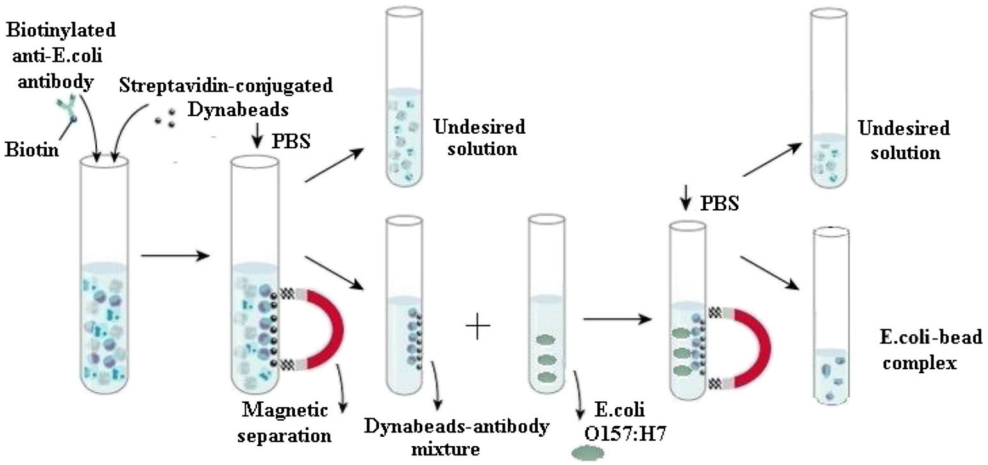

Fig. 4 Preparation processes of the E. coli -Dynabeads complexes

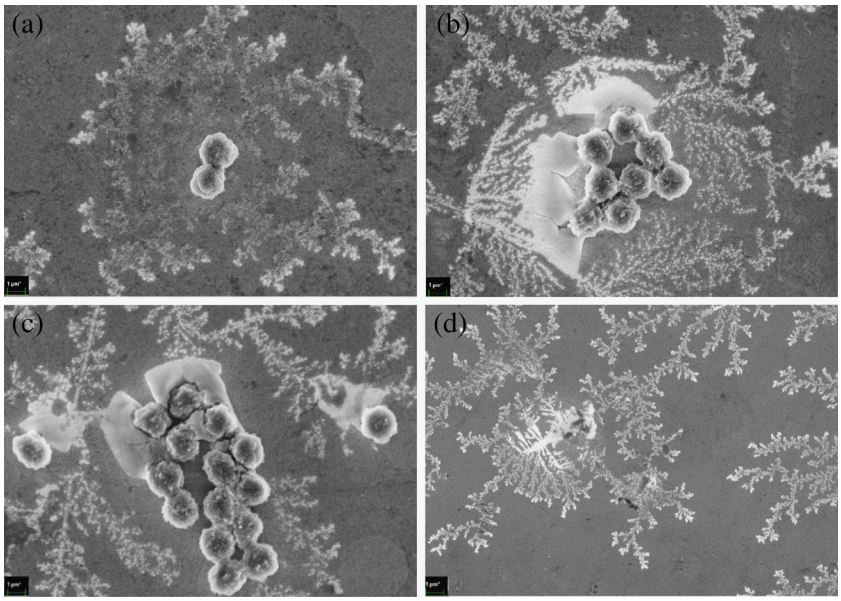

Fig. 5 SEM characterizations of E. coli-conjugated Dynabeads at different concentration (**a**) 100 cfu/ml; **b** 300 cfu/ml; **c** 500 cfu/ml and **d** shigella-Dynabeads

3 Results and discussion

In the previous work of my group, enhancement of GMI effect with a meander structure was investigated by Chen (Chen et al. 2009), and the influence of structural parameters on GMI effect was observed by Wang (Wang et al. 2012). So we designed the meander-shaped GMI sensor with ten turns and appropriate structural parameters in order to obtain the high performance in this work. The GMI ratio of the fabricated sensor was studied, and the maximum GMI ratio was 289.5 %. From a practical point of view, the sensitivity was estimated and the maximum was 19.3 %/Oe at 2.4 MHz.

The GMI ratios with shigella did not change and was not shown here. The GMI ratios measured with and without E. coli were treated as detection value and datum value, respectively. In the testing, the E. coli sample with different concentrations were placed on the top of the sensor respectively. The GMI ratios obtained near the anisotropy field (H_k) were shown in Fig. 7. Evidently, the GMI ratios had risen in varing degrees due to the presence of E. coli samples with different concentrations on the top of GMI sensor. It was worthwhile to note that the GMI ratio increased with increasing the concentration of E. coli. Because different concentration of E. coli were combination with different numbers of Dynabeads as can be seen in Fig. 5. In our early report (Wang et al. 2014a, b), the GMI ratio was improved owing to the presence of superparamagnetic beads on the surface of the sensor, and it was found that high field sensitivity in detection of magnetic beads can be obtained near H_k, the present result was in agreement with it. Many similar researches were also reported (Kurlyandskaya et al. 2003; Devkota et al. 2013) previously, and related theories were put forward to explain the phenomenon. Kurlyandskaya suggested that the presence of the Dynabeads may change the superposition of the constant applied field and the alternating field, thereby changing the

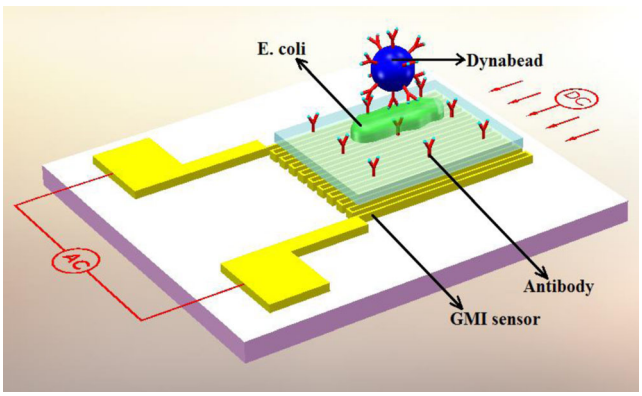

Fig. 6 The GMI biosensor for detection of E. coli O157:H7

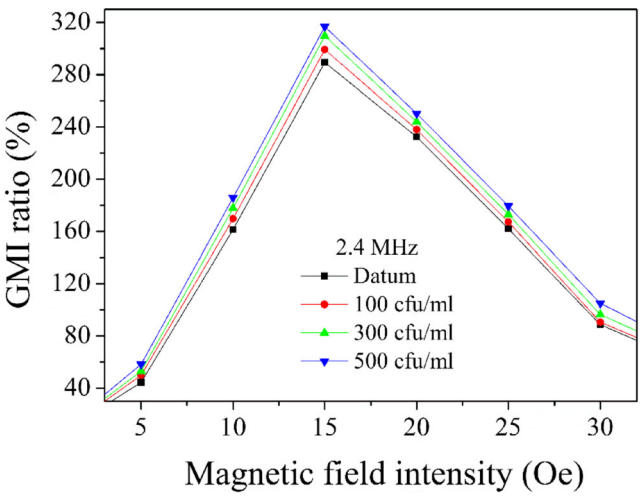

Fig. 7 Field dependence of GMI responses at f =2.4 MHz under the different concentration of Escherichia coli O157:H7

magnetic charge distribution near the surface of the sensing element, the GMI effect was thus enhanced.

The GMI ratio increased first and then decreased as H_{ex} increased. This can be explained in terms of magnetization rotation model (Panina and Mohri 1994): the rotational magnetic permeability related to the GMI effect was first increased and then decreased with increasing H_{ex}, the maximum permeability was achieved as $H_{ex}=H_k$. The AC frequency dependence of the GMI ratio with and without E. coli samples was shown in Fig. 8. When the E. coli sample with different concentrations were placed on the surface of GMI sensor, obviously, there was a small change of the GMI ratio at lower frequency but large change of the GMI ratio occured at high frequency. The greatest change of GMI ratio had taken place near the frequency at which the GMI ratio reaches the maximum, there was an increase of 27.4 % at f=2.4 MHz when the E. coli sample with the concentration of 500 cfu/ml was on the surface of the sensor. The all GMI ratios firstly increased and then decreased with the increasing of frequency. This was because that the GMI effect originated mainly from the skin effect owing to a strong change in the effective permeability caused by the applied DC magnetic field. In the case of small skin effect at low frequency, the sensing element were insensitive to the fringe field. However, both the domain wall motion and magnetic moment rotation contributed to the transverse permeability at high frequency.

The utilization of magnetic particles for the capture, separation, and concentration of various analytes was described more than 20 years ago (Guesdon and Avrameas 1977; Haukanes and Kvam 1993). Irwin (Irwin et al. 2002) investigated immune-magnetic bead mass transport and capture efficiency at low target cell densities in phosphate-buffered saline, the experiment employed beads with the number of 6.7×10^5 to 2.9×10^7 to mixed with low density target cell, the results found that even at low target cell densities ($\leq$70 cfu mL^{-1}), nearly 100 % of the bacteria were captured. Tu (Tu et al. 2003) detected magnetic beads captured Escherichia coli O157:H7 using time-resolved fluoroimmunoassay, the sensitivity of the trf-delfia detection was got and expressed by the fitting equation log CPS= 0.511× log (cfu/mL)+2.625, r^2=0.954 (CPS was the counts per second) in the research. In addition, Tu (Tu et al. 2001) used immunomagnetic beads of different size and antibody conjugating chemistry to capture the Escherichia o157:H7, the capture efficiency of different E,coli strains by different-size beads was observed. Based on the reports as mentioned above, we calculated the number of Dynabeads associated to one E. coli. The percentage of binding between biotinylated anti-E. coli polyclonal antibodies and streptavidin-coupled Dynabeads was regarded as 16 % (Tu et al. 2001), and the gross of used Dynabeads was 10^7 in our experiment. So 40 μl of E. coli-Dynabeads contained 6.4×10^4 Dynabeads. 100 E. coli (1 ml of 100 cfu/mL) was supposed to be captured by Dynabeads, according to the fitting equation (Tu et al. 2003), 4436 E. coli should be detected and one E. coli combined with 14 Dynabeads. Using the same method, we considered the E. coli samples of 100 cfu/ml, 300 cfu/ml and 500 cfu/ml approximately consisted of 1400 2400 and 3100 Dynabeads respectively.

Figure 9 showed the mean of GMI ratio for 10 repeated measurements of the different concentration of the E. coli O157:H7. Obviously, the GMI ratio was greatly increased in the presence of E.coli sample, and increased as the concentration of E. coli increased. When the samples with 100, 300 and 500 E. coli were employed, the increases were 9.7, 20.5 and 27.4 %, respectively. In this case, the lower concentration of 100 cfu/ml can be successfully detected, which indicated that sensitive detection of E. coli using the GMI-based biosensor was fully realized. Compared with conventional enzyme-linked immunosorbent assay method, which usually cost several days, the GMI-based biosensor is notably simple and

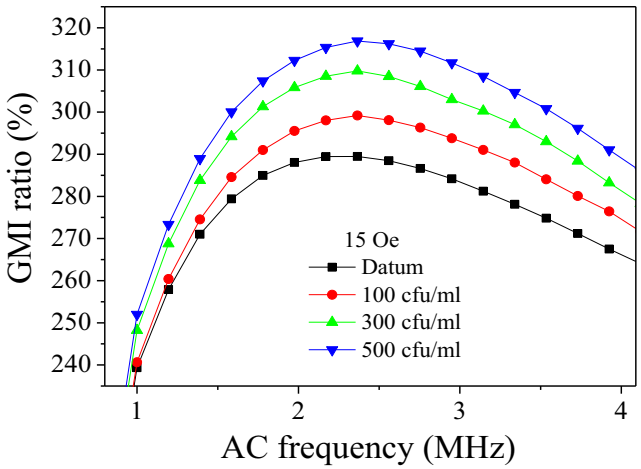

Fig. 8 Frequency dependence of GMI responses at H_{ex} =15 Oe under the different concentration of Escherichia coli O157:H7

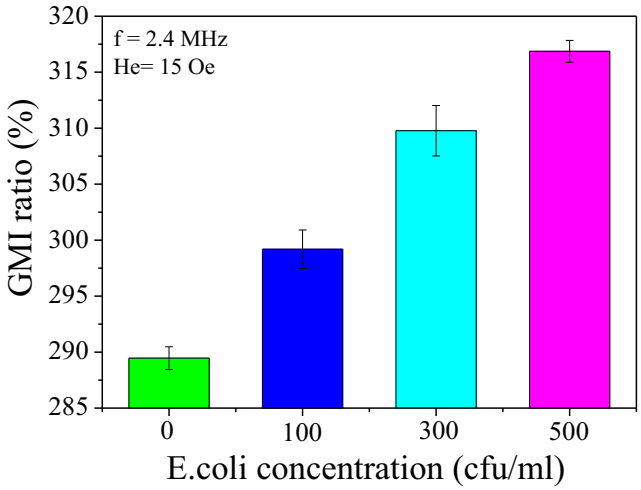

Fig. 9 GMI change in relation to the concentration of the Escherichia coli O157:H7

rapid. Compared with other biosensor, the minimum detectable concentration of 1.2×10^3 cells/ml is achieved by a MR sensor (Oh et al. 2013), and as low as 1.6×10^2 to 1.2×10^3 cells of E. coli O157:H7 cells in pure culture and ground beef sample can be detected using a label-free, microfluidics and interdigitated array microelectrode-based impedance biosensor (Varshney et al. 2007). The GMI-based biosensor in this work possesses lower minimum detectable concentration of 100 cfu/ml. This can be attributed to the unique advantage of the GMI sensor, namely, the frequency-sensitive inductance contributes to magnetoimpedance. Especially the mutual inductance of flexural sandwich structure was ultrasensitive at high frequencies. In addition, the relative standard deviation (RSD) is 0.95 % for successive measurements of 10 times (100 cfu/ml) under same testing conditions, which indicates a good precision. The high stability of GMI sensor contributes the reliability of measurement results. In our early report (Wang et al. 2014a, b), 90 streptavidin-coupled Dynabeads can be detected by the GMI sensor, however 1400 Dynabeads in 100 cfu/ml E.coli Is detected. So in theory the detection limit should be below 100 cfu/ml. Tu (Tu et al. 2001, 2009) observed the factors affecting the bacterial capture efficiency, the heavier and larger diameter Dynabeads exhibited a better efficiency in capturing the bacteria. The factors affecting the capture efficiency would certainly be related the number of Dynabeads combined with E. coli. It will be further studied next.

In addition, the distance between the sensing elements and E. coli sample can be decreased to a lower extent through integration technology. Because the distance affected the fringe field of Dynabeads. Consequently, developing of a high-integrated GMI biosensor (Wang et al. 2014a, b) may be of great use in ultrasensitive detection of biological markers, especially to some early diagnosis and treatment of some diseases such as mammary cancer, prostatic cancer and so on.

4 Conclusions

In this work, a GMI-based biosensor was developed for detection of E. coli O157:H7. The GMI sensor was fabricated by MEMS technology. A separate Au film substrate as immunoplatform was used to capture E. coli O157:H7. The monoclonal mouse anti-E. coli antibody was immobilized Au film substrate surface with a self-assembled layer. The different concentration E. coli O157:H7 (100, 300 and 500 cfu/ml, 1 ml) were combined with DAC respectively. DAC were prepared by conjugating streptavidin-coupled Dynabeads with biotin-labeled polyclonal mouse anti-E. coli antibodies. The classical sandwich assay was used for detection of E. coli O157:H7 targeted with Dynabeads by using antibody-antigen pair combination of biotin-streptavidin. The fundamental principle for detection of E. coli O157:H7 based on GMI sensor was that Dynabeads were employed as magnetic labels of E. coli O157:H7, and E. coli O157:H7 can be monitored by detecting the fringe field of Dynabeads using magnetic sensing elements. Experimental results showed that the GMI ratios increased as the E. coli concentration increased. A lower detectable concentration of 100 cfu/ml was achieved in present work. From the viewpoint of minimum detectable Dynabeads concentration (Wang et al. 2014a, b), the detection limit should be below 100 cfu/ml in theory. In further studies, we will focus on detection research of the lower E. coli O157:H7 concentration (<100 cfu/ml) on the basis of factors affecting the E. coli capture efficiency of immune beads, such as size、density、concentration of Dynabeads. And we will consider integrating the GMI sensing elements and immunoplatform to establish a high integrated GMI-based biosensing system. The GMI-based biosensor provides a new method to rapid and sensitive detection of E. coli O157:H7, which has a large potential for bio-application.

Acknowledgments This work was supported by The National Natural Science Foundation of China (No. 61074168 and No. 61273065), National Science and Technology Support Program (2012BAK08B05) and National Key Laboratory Research Fund (9140C790403110C7905). Natural Science Foundation of Shanghai (13ZR1420800) and the Analytical and Testing Center in Shanghai Jiao Tong University.

References

F. Alves, L. Abi Rached, J. Moutoussamy, C. Coillot, Sens. Actuators A **142**, 459 (2008)

F.E. Atalay, H. Kaya, S. Atalay, J. Phys. D, Appl. Phys. **39**, 431 (2006)

C. Berggren, B. Bjarnason, G. Johansson, Biosens. Bioelectron. **13**, 1061–1068 (1998)

R.L. Bunchnan, M.P. Dolye, Food Technol. **51**, 69–76 (1997)

Centers for Disease Control and Prevention (CDC), 2005. Disease Information-E. coli O157:H7. Available at: www.cdc.gov. Accessed December.

L. Chen, Y. Zhou, Z.M. Zhou, W. Ding, J. Phys. D. Appl. Phys. **42**, 145005 (2009)

L. Chen, C.C. Bao, H. Yang, C. Lei, Y. Zhou, D.X. Cui, Biosens. Bioelectron. **26**, 3246–3253 (2011)

D.R. Demarco, E.W. Saaski, D.A. McCare, D.V. Lim, J. Food Prot. **62**, 711–716 (1999)

J. Devkota, A. Ruiz, P. Mukherjee, H. Srikanth, M.H. Phan, IEEE Trans. Magn. **49**, 4060 (2013)

K.S. Gracias, J.L. McKillip, J. Can, Microbiol. **50**, 883–890 (2004)

J.L. Guesdon, S. Avrameas, Magnetic solid phase enzymeimmunoassay. Immunochemistry **14**, 443–447 (1977)

B.-I. Haukanes, C. Kvam, Application of magnetic beads in bioassays. Biohechnol. **12**, 60–63 (1993)

S.S. Iqbal, W.M. Mayo, J.G. Bruno, B.V. Bronk, C.A. Batt, J.P. Chambers, Biosens. Bioelectron. **15**, 549–578 (2000)

P. Irwin, W. Damert, J. Berwater, A. Gehring, S.-I. Tu, J. Rapid Meth, Autom. Microbiol. **10**, 129–147 (2002)

D. Ivniski, I. Abdel-Hamid, P. Atanasov, E. Wilkins, Biosens. Bioelectron. **14**, 599–624 (1999)

G.V. Kurlyandskaya, M.L. Sanchez, B. Hernando, V.M. Prida, P. Gorria, M. Tejedor, Appl. Phys. Lett. **82**, 3053–3055 (2003)
D.P. Makhnovskiy, L.V. Panina, Sens. Actuators A **81**, 91 (2000)
V. E. Makhotkina, B. P. Shurukhina, V. A. Lopatina, P. Yu. Marchukova, Yu. K. Levina, Sens. actuators A 25–27, 759 (1991).
C.S. Mayo, R.B.J. Hallock, Immunol. Methods. **120**, 105–114 (1989)
S. Oh, M. Jadhav, J. Lim, V. Reddy, C. Kim, Biosens. Bioelectron. **41**, 758–763 (2013)
L.V. Panina, K. Mohri, Appl. Phys. Lett. **65**, 1189 (1994)
M.H. Phan, H.X. Peng, M.R. Wisnom, S.C. Yu, N.H. Nghi, C.G. Kim, Sens. Actuators A **129**, 62 (2006)
C.A. Phillips, J. Sci. Food Agric. **79**, 1367–1381 (1999)
C. Ruan, L. Yang, Y. Li, Anal. Chem. **74**, 4814–4820 (2002)
T.M. Silk, C.W.J. Donnelly, Food Protection **60**, 1483–1486 (1997)
P.D. Skottrup, M. Nicolaisen, A.F. Justesen, Biosens. Bioelectron. **24**, 339–348 (2008)
R.L. Sommer, C.L. Chine, Appl. Phys. Lett. **47**, 3346 (1995)
T.C. Tang, A.P. Deng, H.J. Huang, Anal. Chem. **74**, 2617–2621 (2002)
S.-I. Tu, M. Golden, P. Andreotti, L.S.L. Yu, P. Irwin, J. Rapid Meth, Autom. Microbiol. **9**, 71–84 (2001)
S.-I. Tu, J. Uknalis, M. Gore, P. Irwin, I. Feder, J. Rapid Meth, Autom. Microbiol. **11**, 35–46 (2003)
S.-I. Tu, S. Reed, A. Gehring, Y. He, G. Paoli, Sensors **9**, 717–730 (2009)
M. Varshney, Y. Li, B. Srinivasan, S. Tung, Sens. Actuators B. **128**, 99–107 (2007)
M. Vázquez, M. Knobel, M.L. Sánchez, Sens. Actuators A **159**, 20–29 (1997)
J. Wang, P.V.A. Pamidi, K.R. Rogers, Anal. Chem. **70**, 1171–1175 (1998)
T. Wang, C. Lei, J. Lei, Z. Yang, Y. Zhou, Appl. Phys. A **109**, 205–211 (2012)
T. Wang, Y. Zhou, C. Lei, J. Lei, Z. Yang, Sens. Actuators B **186**, 727–733 (2013)
T. Wang, Z. Yang, C. Lei, J. Lei, Y. Zhou, Biosens. Bioelectron. **58**, 338–344 (2014a)
T. Wang, Z. Yang, C. Lei, J. Lei, Y. Zhou, J. Appl. Phys. **115**, 223901 (2014b)
T. Wink, S.J. Van Zuilen, A. Bult, W.P. Van Bennekom, Anal. Chem. **70**, 827–832 (1998)
A. Wolter, R. Niessner, M. Seidel, Anal. Chem. **80**, 5854–5863 (2008)
L. Yang, R. Bashir, Biotechnol. Adv. **26**, 135–150 (2008)
L.S.L. Yu, J. Uknalis, S.J. Tu, Immunol. Methods. **256**, 11–18 (2001)
Y. Zhou, J.Q. Yu, X.L. Zhao, B.C. Cai, J. Appl. Phys. **89**, 1961 (2001)